Ecoulements Compressibles Diphasiques avec Raffinement de Maillage Automatique

Two-fluid Compressible Flows with Multiresolution Adaptive Mesh Refinement

Gen Wu

Supervisors: Nicolas Grenier, Caroline Nore

LISN, Université Paris-Saclay

gen.wu@upsaclay.fr

GDR TRANSINTER PHASE DEUX, September 25, 2024

Motivation

Crucial role of **boiling** in optimizing thermal performance in various industrial scenarios

Challenges of **two-phase flow modelling** (phase change, surface tension……)

Use **adaptive mesh refinement** strategy to improve efficiency and flexibility

Flows of interest

⁎ compressible gas + incompressible liquid

⁎ low Mach regime $M \ll 1$

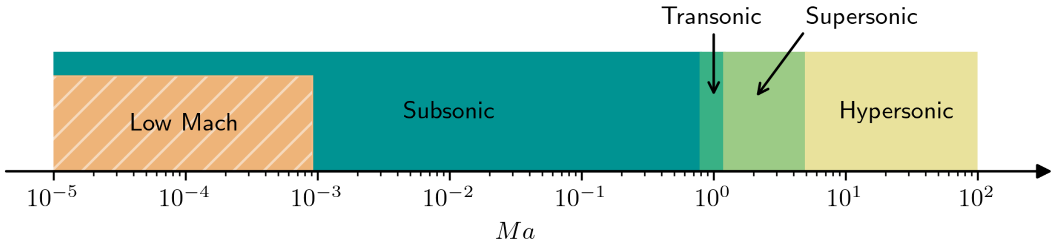

Objective: develop a **compressible** solver for liquid-gas flows

- ✓ Accurate in interface capturing
- ✓ Accurate in the low Mach regime
- ✓ Capable of handling heat transfer and phase change
- ✓ Integrated with an effective adaptive mesh refinement technique

Governing equations

Each phase is described by a compressible model

$$\begin{cases} \partial_t \rho + \nabla \cdot (\rho \mathbf{u}) = 0 \\ \partial_t (\rho \mathbf{u}) + \nabla \cdot (\rho \mathbf{u} \otimes \mathbf{u}) + \nabla p = \nabla \cdot \mathbb{S} + \rho \boldsymbol{f} \\ \partial_t (\rho E) + \nabla \cdot ((\rho E + p)\mathbf{u}) = \nabla \cdot (\mathbb{S}\mathbf{u}) + \rho \boldsymbol{f} \cdot \boldsymbol{u} + \nabla \cdot (\mathscr{K} \nabla T) \end{cases}$$

ρ	fluid density	p	fluid pressure	$\boldsymbol{f}$	volume forces	$\mathscr{K}$	thermal conductivity
$\boldsymbol{u}$	fluid velocity	$\mathbb{S}$	viscous stress tensor	E	total energy	c	speed of sound

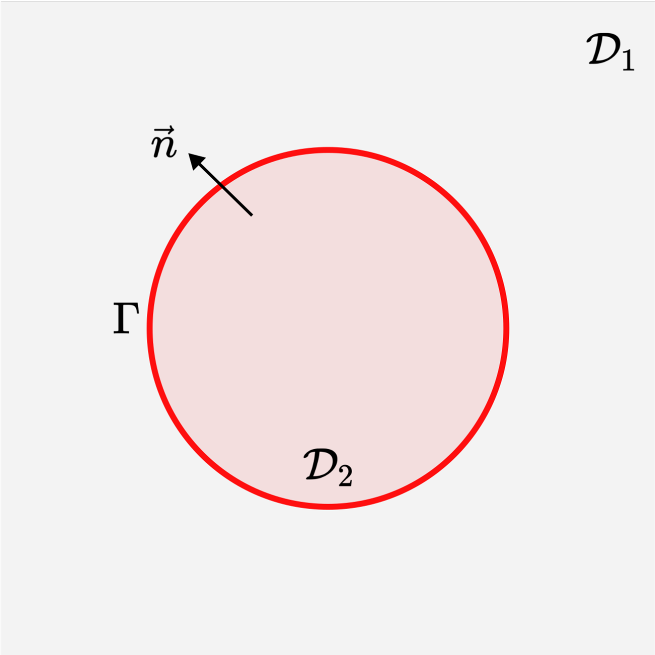

Equation of state

Ex: stiffened gas EOS, barotropic EOS

Interface jump conditions

✓ mass conservation → **velocity jump**

$$[\![\mathbf{u}\cdot\mathbf{n}]\!]_\Gamma = \dot{m}[\![\frac{1}{\rho}]\!]_\Gamma$$

✓ momentum balance → **pressure jump**

$$[\![p]\!]_\Gamma = \sigma\kappa$$

✓ energy conservation → **thermal flux jump**

$$[\![\mathscr{K}\nabla T]\!]_\Gamma \cdot \mathbf{n} = \dot{m}L_{\text{heat}}$$

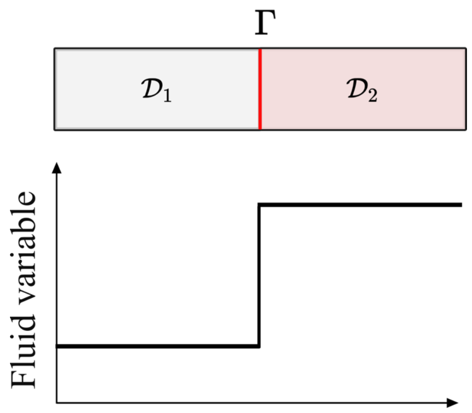

$\dot{m}$ phase change mass flow rate

L_{heat} latent heat of vaporization

$[\![\,\cdot\,]\!]_\Gamma$ jump operator across the interface

Interface description: level set method

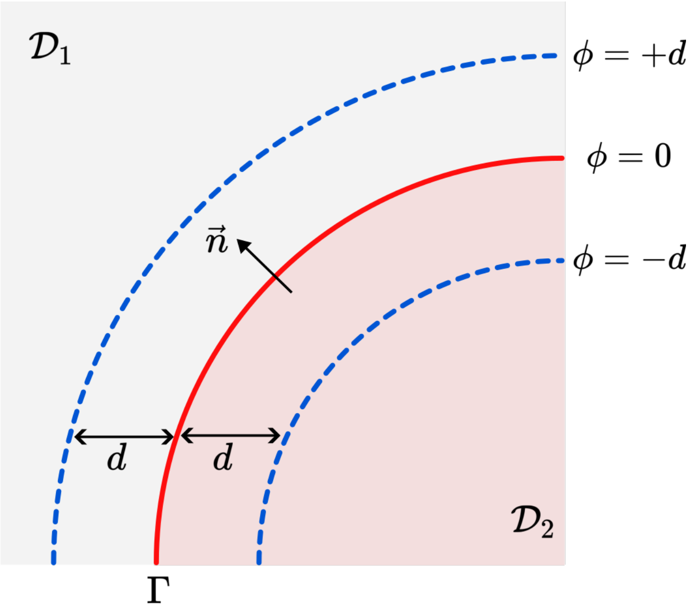

Level set function

$$\phi = \begin{cases} d(\mathbf{x}, \Gamma) & \text{for } \mathbf{x} \in \mathcal{D}_1, \\ 0 & \text{for } \mathbf{x} \in \Gamma, \\ -d(\mathbf{x}, \Gamma) & \text{for } \mathbf{x} \in \mathcal{D}_2. \end{cases}$$

Level set advection

$$\partial_t \phi + \mathbf{u}_\Gamma \cdot \nabla \phi = 0$$

interface $\Gamma(t) = \{\mathbf{x} \in \mathcal{D} \mid \phi(\mathbf{x}, t) = 0\}$

interface velocity $\mathbf{u}_\Gamma$

normal vector $\mathbf{n} = \dfrac{\nabla \phi}{|\nabla \phi|}$

interface curvature $\kappa = \nabla \cdot \left(\dfrac{\nabla \phi}{|\nabla \phi|} \right)$

Discretization 5th order One-Step scheme

[V. Daru et al., 2004, Zou et al., 2020]

distance property $|\nabla \phi| = 1$

Reinitialization (redistancing) $\partial_\tau \phi = \text{sign}(\phi_0)(1 - |\nabla \phi|)$

Numerical method

Finite Volume discretization

A single fluid Lagrange-Projection type scheme [C. Chalons et al., 2016]

Decomposition of the global system into 3 subsystems

$$\begin{cases} \partial_t \rho & \underbrace{+\, \rho \nabla \cdot \mathbf{u}} & \underbrace{+\, \mathbf{u} \cdot \nabla \rho} & = 0 & \\ \partial_t (\rho \mathbf{u}) & +\, \rho \mathbf{u} \nabla \cdot \mathbf{u} + \nabla p & +\, \mathbf{u} \cdot \nabla (\rho \mathbf{u}) & = \rho \boldsymbol{f} & +\, \nabla \cdot \mathbb{S} \\ \partial_t (\rho E) & +\, \rho E \nabla \cdot \mathbf{u} + \nabla \cdot (p \mathbf{u}) & +\, \mathbf{u} \cdot \nabla (\rho E) & = \rho \boldsymbol{f} \cdot \mathbf{u} & +\, \nabla \cdot (\mathbb{S} \mathbf{u}) + \nabla \cdot (\mathscr{K} \nabla T) \\ \partial_t \phi & & +\, \mathbf{u}_\Gamma \cdot \nabla \phi & = 0 & \end{cases}$$

Acoustic | **Transport** | **Diffusion**

$$\begin{bmatrix} \rho \\ \rho \mathbf{u} \\ \rho E \\ \phi \end{bmatrix}^{n} \Rightarrow \begin{bmatrix} \rho \\ \rho \mathbf{u} \\ \rho E \\ \phi \end{bmatrix}^{n+1-} \Rightarrow \begin{bmatrix} \rho \\ \rho \mathbf{u} \\ \rho E \\ \phi \end{bmatrix}^{n+} \Rightarrow \begin{bmatrix} \rho \\ \rho \mathbf{u} \\ \rho E \\ \phi \end{bmatrix}^{n+1}$$

$t = n\Delta t$ $\qquad\qquad$ $t = (n+1)\Delta t$

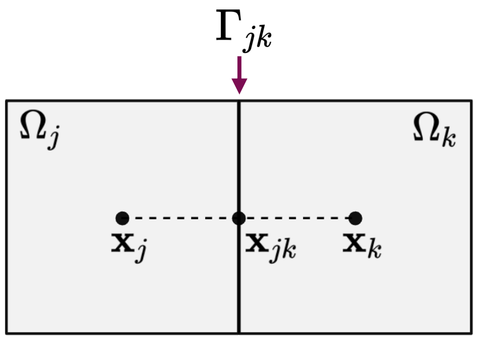

Step 1. Acoustic step [C. Chalons et al., 2016]

$$\begin{bmatrix}\rho\\ \rho\mathbf{u}\\ \rho E\\ \phi\end{bmatrix}^{n} \Rightarrow \begin{bmatrix}\rho\\ \rho\mathbf{u}\\ \rho E\\ \phi\end{bmatrix}^{n+}$$

Godunov approach

$$L_j\rho_j^{n+} = \rho_j^n,$$

$$L_j(\rho\mathbf{u})_j^{n+} = (\rho\mathbf{u})_j^n - \frac{\Delta t}{|\Omega_j|}\sum_{k\in\mathcal{N}(j)}|\partial\Omega_{jk}|\pi_{jk}^*\mathbf{n}_{jk} - \Delta t\{\rho\nabla\Psi\}_j,$$

$$L_j(\rho E)_j^{n+} = (\rho E)_j^n - \frac{\Delta t}{|\Omega_j|}\sum_{k\in\mathcal{N}(j)}|\partial\Omega_{jk}|\pi_{jk}^*u_{jk}^* - \Delta t\{\mathbf{u}^*\rho\nabla\Psi\}_j,$$

$$\phi_j^{n+} = \phi_j^n,$$

$$L_j = 1 + \frac{\Delta t}{|\Omega_j|}\left(\sum_{k\in\mathcal{N}(j)}|\partial\Omega_{jk}|u_{jk}^*\right).$$

π surrogate pressure from Suliciu-type relaxation

Approximate Riemann solver

Numerical flux for bulk cells

$$u_{jk}^* = \frac{\mathbf{n}_{jk}\cdot(a_j\mathbf{u}_j + a_k\mathbf{u}_k)}{a_j + a_k} - \frac{\pi_k - \pi_j}{(a_j + a_k)}$$

$$\pi_{jk}^* = \frac{a_k\pi_j + a_j\pi_k}{a_j + a_k} + \frac{a_j a_k}{a_j + a_k}\mathbf{n}_{jk}\cdot(\mathbf{u}_j - \mathbf{u}_k)$$

for interface cells (+ jump conditions)

$$u_{jk}^* = \frac{\mathbf{n}_{jk}\cdot\left(a_j\mathbf{u}_j + a_k\mathbf{u}_k + a_k[\![\mathbf{u}]\!]_{\Gamma_{jk}}\right)}{a_j + a_k} + \frac{\pi_j - \pi_k - [\![p]\!]_{\Gamma_{jk}}}{a_j + a_k}$$

$$\pi_{jk}^* = \frac{a_k\pi_j + a_j\pi_k + a_j[\![p]\!]_{\Gamma_{jk}}}{a_j + a_k} + \frac{a_j a_k}{a_j + a_k}\mathbf{n}_{jk}\cdot\left(\mathbf{u}_j - \mathbf{u}_k - [\![\mathbf{u}]\!]_{\Gamma_{jk}}\right)$$

$$a_j = 1.1\rho_j c_j, a_k = 1.1\rho_k c_k$$

Low Mach analysis

Low Mach regime $\tilde{\nabla}\tilde{p} = \mathcal{O}(M^2)$

Truncation errors of the dimensionless acoustic subsystem in the low Mach regime

$$\begin{cases} \partial_{\tilde{t}}\tilde{\rho} + \tilde{\nabla}\cdot\tilde{\mathbf{u}} = \mathcal{O}(\Delta\tilde{t}) + \mathcal{O}(M\Delta\tilde{x}), \\ \partial_{\tilde{t}}(\tilde{\rho}\tilde{\mathbf{u}}) + \tilde{\rho}\tilde{\mathbf{u}}\tilde{\nabla}\cdot\tilde{\mathbf{u}} + \dfrac{1}{M^2}\tilde{\nabla}\tilde{p} = \mathcal{O}(\Delta\tilde{t}) + \mathcal{O}(\dfrac{\Delta\tilde{x}}{M}), \\ \partial_{\tilde{t}}(\tilde{\rho}\tilde{E}) + \tilde{\rho}\tilde{E}\tilde{\nabla}\cdot\tilde{\mathbf{u}} + \tilde{\nabla}\cdot(\tilde{p}\tilde{\mathbf{u}}) = \mathcal{O}(\Delta\tilde{t}) + \mathcal{O}(M\Delta\tilde{x}). \end{cases}$$

Dimensionless variables

$$\tilde{\rho} = \rho/\hat{\rho}_i, \quad \tilde{p} = p/\hat{p}_i, \quad \tilde{c} = c/\hat{c}_i, \quad \tilde{e} = e/\hat{e}_i, \quad i = 1, 2$$

Asymptotic expansion

$$p(t,\mathbf{x}) = M^0 p^{(0)}(t,\mathbf{x}) + M^1 p^{(1)}(t,\mathbf{x}) + M^2 p^{(2)}(t,\mathbf{x}) + \cdots$$

Low Mach correction [Z. Zou et al., 2022]

$$u_{jk}^{*,\theta} = (1-\theta_{jk})\left(\mathbf{n}_{jk}\cdot\frac{\mathbf{u}_j + \mathbf{u}_k + [\![\mathbf{u}]\!]_{\Gamma_{jk}}}{2} + \frac{\pi_j - \pi_k - [\![p]\!]_{\Gamma_{jk}}}{a_j + a_k}\right) + \theta_{jk}u_{jk}^*$$

$$\pi_{jk}^{*,\theta} = (1-\theta_{jk})\frac{\rho_k\pi_j + \rho_j\left(\pi_k + [\![p]\!]_{\Gamma_{jk}}\right)}{\rho_j + \rho_k} + \theta_{jk}\pi_{jk}^*$$

$$\theta_{jk} = \min\left(\frac{u_{jk}^*}{\max(c_j, c_k)}, 1\right)$$

uniform truncation error
with respect to Mach number

Step 2. Transport step

$$\begin{bmatrix} \rho \\ \rho \mathbf{u} \\ \rho E \\ \phi \end{bmatrix}^{n+} \Rightarrow \begin{bmatrix} \rho \\ \rho \mathbf{u} \\ \rho E \\ \phi \end{bmatrix}^{n+1-}$$

Upwind scheme + ghost fluid method (linear extrapolation)

$$\partial_t b + \nabla \cdot (b\mathbf{u}) + b\nabla \cdot \mathbf{u} = 0 \qquad b = (\rho, \rho u, \rho v, \rho E)^{\mathbf{T}}$$

$$b_j^{n+1-} = b_j^{n+} - \frac{\Delta t}{|\Omega_j|} \sum_{k \in \mathcal{N}(j)} |\partial \Omega_{jk}| u^*_{jk} b^{n+}_{jk} + b_j^{n+} \frac{\Delta t}{|\Omega_j|} \sum_{k \in \mathcal{N}(j)} |\partial \Omega_{jk}| u^*_{jk}$$

$$b^{n+}_{jk} = \begin{cases} b_j^{n+} & \text{if } u^*_{jk} > 0, \\ b_k^{n+} & \text{if } u^*_{jk} \leq 0 \text{ and } \phi_j \phi_k > 0, \\ b^{n+}_{k,ghost} & \text{if } u^*_{jk} \leq 0 \text{ and } \phi_j \phi_k < 0. \end{cases}$$

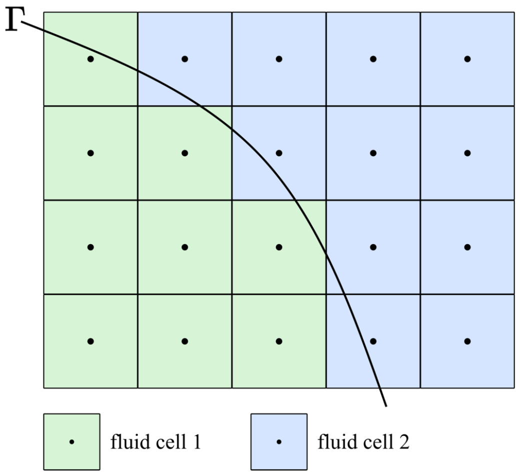

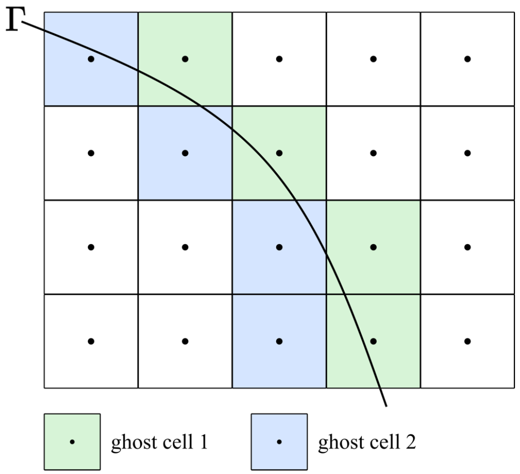

Step 3. Diffusion step

Discretization of **viscous diffusion** Centered second-order FV method

$$\begin{bmatrix}\rho\\ \rho\mathbf{u}\\ \rho E\\ \phi\end{bmatrix}^{n+1-} \Rightarrow \begin{bmatrix}\rho\\ \rho\mathbf{u}\\ \rho E\\ \phi\end{bmatrix}^{n+1}$$

Discretization of **heat diffusion** near the interface

1. **Without phase change**, continuous heat flux across the interface
$$\mathcal{K}_j \frac{T_j - T_{\Gamma_j}}{\Delta x_j^\Gamma} = \mathcal{K}_k \frac{T_{\Gamma_j} - T_k}{\Delta x_k^\Gamma}$$

interface temperature

$$T_{\Gamma_j} = \frac{\mathcal{K}_j T_j \Delta x_k^\Gamma + \mathcal{K}_k T_k \Delta x_j^\Gamma}{\mathcal{K}_j \Delta x_k^\Gamma + \mathcal{K}_k \Delta x_j^\Gamma}$$

heat flux across the interface

$$\mathcal{K}_j \nabla T_{\Gamma_j} \cdot \mathbf{n}_{jk} = \mathcal{K}_j \frac{T_{\Gamma_j} - T_j}{\Delta x_j^\Gamma}$$

2. **With phase change**, discontinuous heat flux

assumption $T_\Gamma = T_{\text{sat}}$

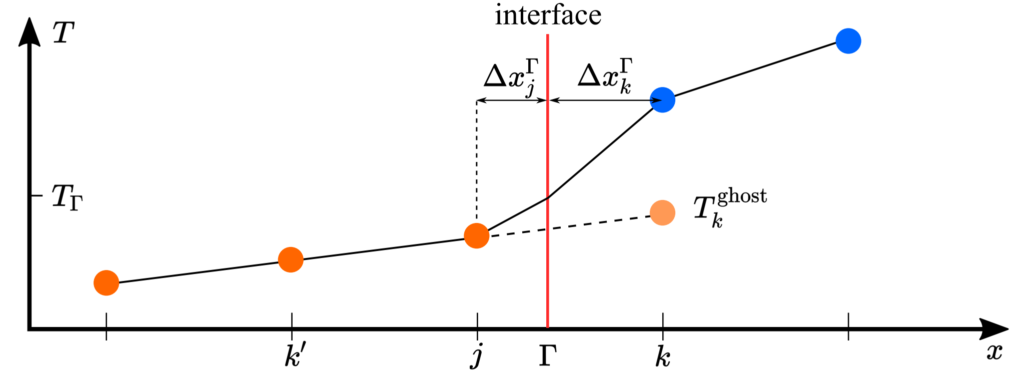

Phase change modeling

Compute phase change mass flow rate from heat flux

[Y. Sato et al., 2013, S. Tanguy et al., 2014]

$$[\![\mathscr{K}\nabla T]\!]_\Gamma \cdot \mathbf{n} = \dot{m} L_{\text{heat}} \quad \Rightarrow \quad \dot{m} = \frac{-k_{\text{liq}} \nabla T_{\text{liq}} \cdot \mathbf{n} + k_{\text{vap}} \nabla T_{\text{vap}} \cdot \mathbf{n}}{L_{\text{heat}}}$$

Compute interface velocity for $\partial_t \phi + \boxed{\mathbf{u}_\Gamma} \cdot \nabla \phi = 0$

$$[\![\mathbf{u} \cdot \mathbf{n}]\!]_\Gamma = \dot{m} [\![\frac{1}{\rho}]\!]_\Gamma \quad \Rightarrow \quad \vec{u}_\Gamma = \vec{u}_{\text{liq}} - \frac{\dot{m}}{\rho_{\text{liq}}} \cdot \mathbf{n} = \vec{u}_{\text{vap}} - \frac{\dot{m}}{\rho_{\text{vap}}} \cdot \mathbf{n}$$

Compute heat flux at the interface

Depends on how to approximate the temperature gradient

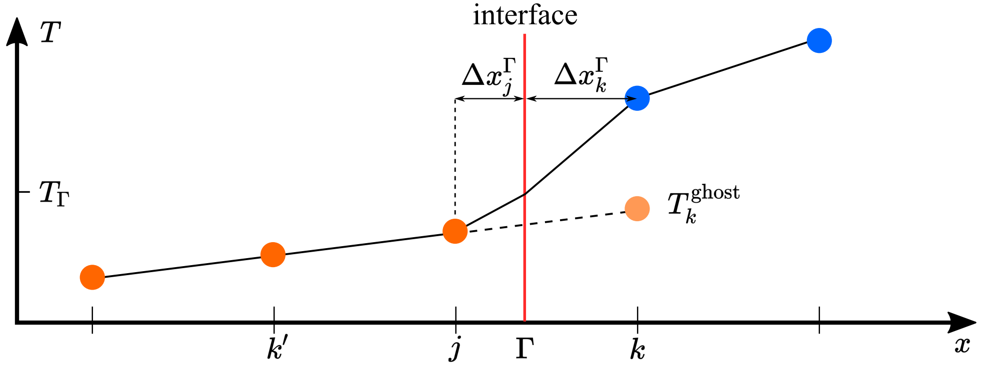

$$T_\Gamma = T_{sat}$$

$$\mathscr{K}_j \nabla T_{\Gamma_j} \cdot \mathbf{n}_{jk} =$$

1. $$\mathscr{K}_j \frac{T_{\text{sat}} - T_j}{\Delta x_j^\Gamma}$$ use interface temperature

2. $$\mathscr{K}_j \frac{T_k^{\text{ghost}} - T_j}{\Delta x_{jk}}$$ use neighboring **ghost cell**

3. $$\frac{1}{2}\mathscr{K}_j \left(3\frac{T_{\text{sat}} - T_{k'}}{\Delta x_{k'j} + \Delta x_j^\Gamma} - \frac{T_j - T_{k'}}{\Delta x_{k'j}} \right)$$ use neighboring cell belonging to the **same fluid** [Z. Zou, 2020]

4. $$\mathscr{K}_j \frac{-\Delta x_j^\Gamma T_{k'} + (\Delta x_j^{\Gamma 2} - \Delta x_{jk}^2) T_j + \Delta x_{jk}^2 T_{\text{sat}}}{\Delta x_{jk} \Delta x_j^\Gamma (\Delta x_{jk} + \Delta x_j^\Gamma)}$$ **second-order** [Y. Sato et al., 2013, L. Anumolu et al., 2018]

Linear sloshing

$a_0/g = 0.01$

$M \approx 10^{-5}$

Property	Gas	Liquid
ρ ($\mathrm{kg \cdot m^{-3}}$)	1	1000
c ($\mathrm{m \cdot s^{-1}}$)	300	1200
g ($\mathrm{m \cdot s^{-2}}$)	10	
a_0 ($\mathrm{m \cdot s^{-2}}$)	0.1	

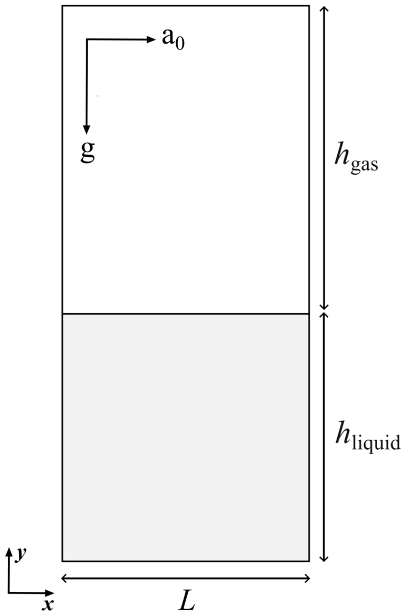

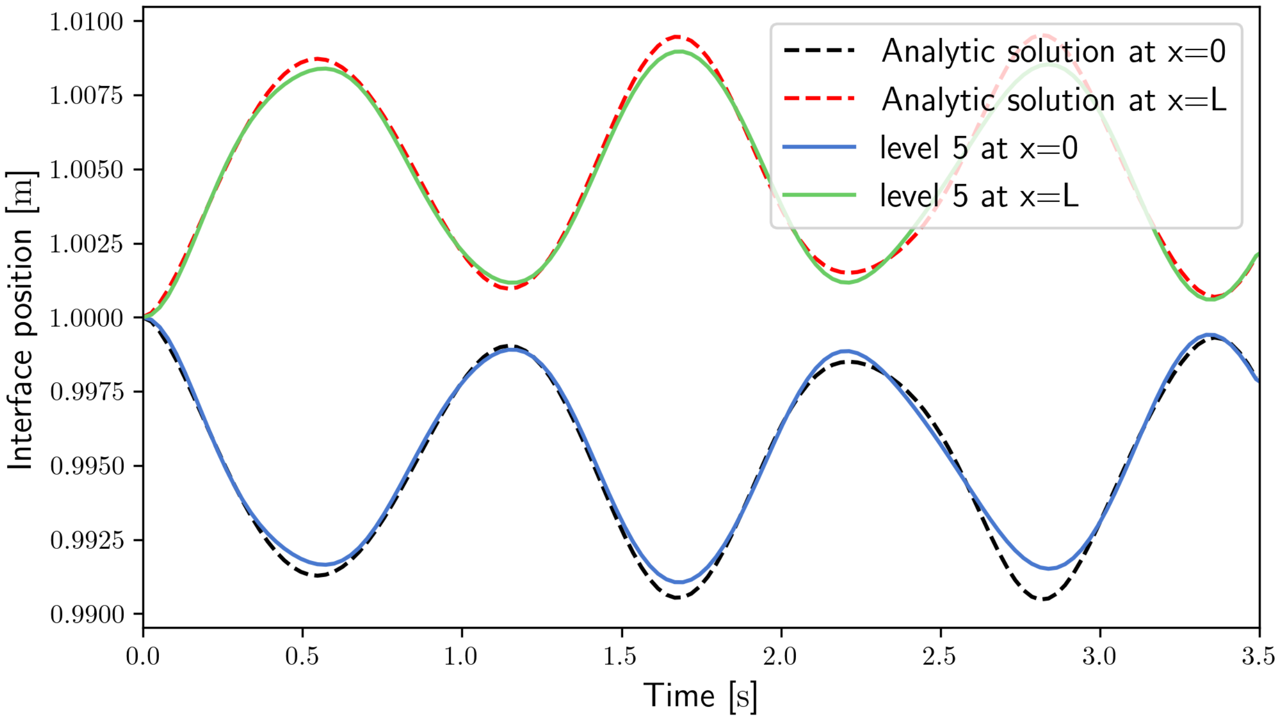

spatial resolution: 32 * 72

Rayleigh-Taylor instabilities

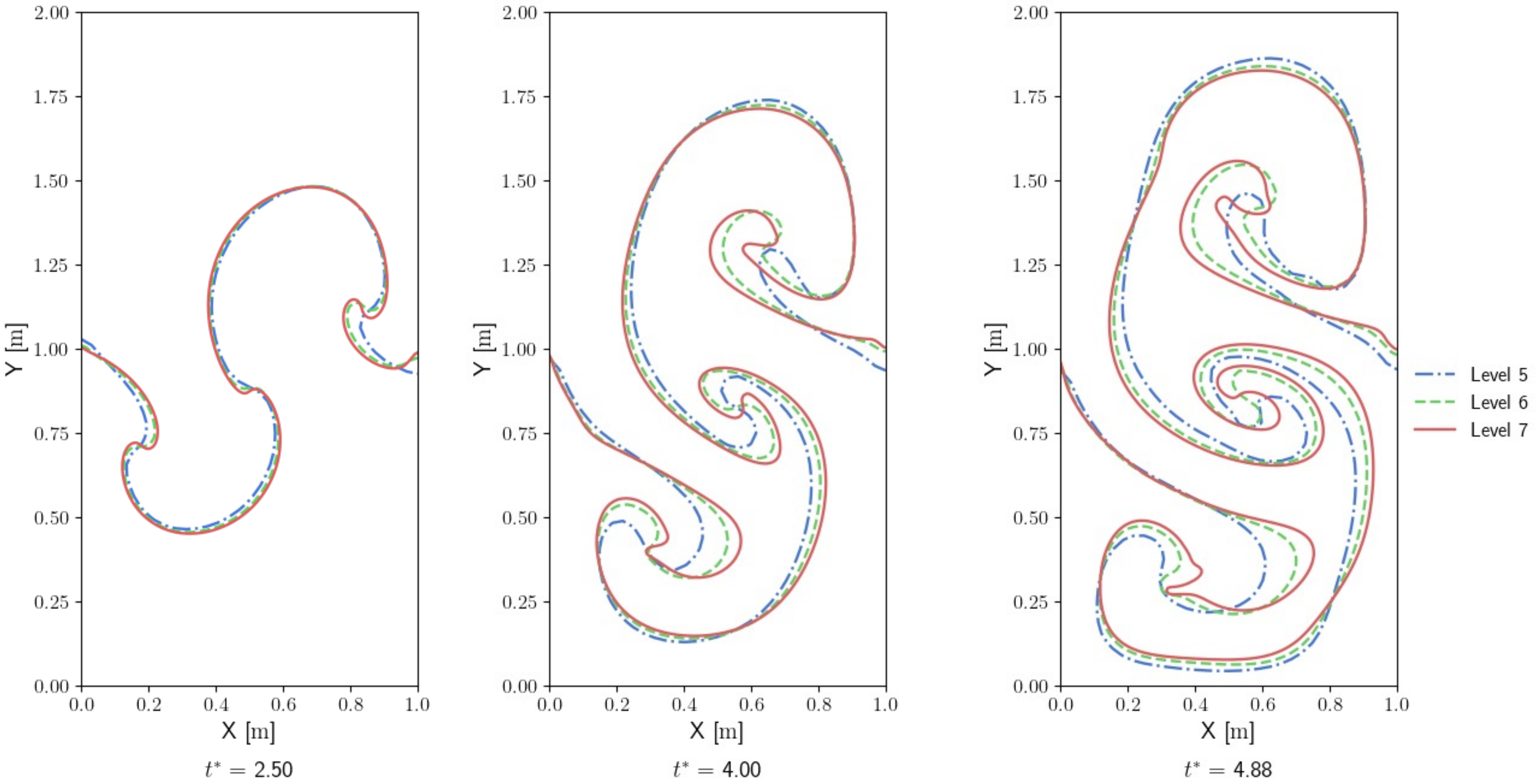

Grid level	Resolution
5	32 * 64
6	64 * 128
7	128 * 256

Property	fluid 1	fluid 2
ρ $(\mathrm{kg}\cdot\mathrm{m}^{-3})$	1.8	1.0
μ $(\mathrm{Pa}\cdot\mathrm{s})$	0.00238	0.00238
γ	7.0	7.0
p (Pa)	400	400
$g_y(\mathrm{m}\cdot\mathrm{s}^{-2})$	1.0	
Re	420	

$Ma < 10^{-3}$

interface initial position:

$$y = 1 - 0.15\sin(2\pi x)$$

1D non-isothermal problem

Oscillation of a liquid layer between two gas pockets [V. Daru et al., 2010]

$M \approx 10^{-3}$

$T_{\text{wall}} = 373.15\text{K}$

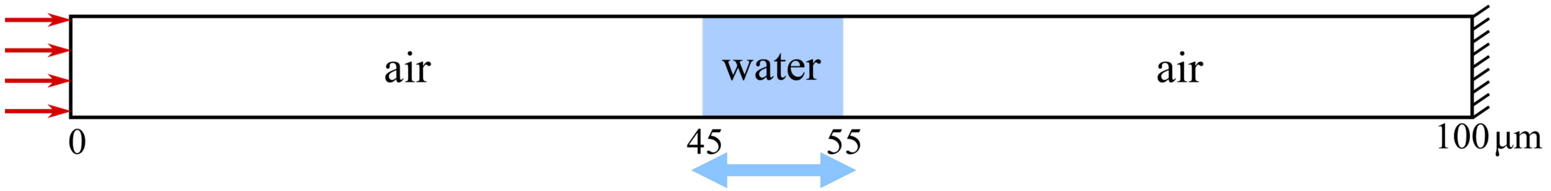

$T_0 = 293.15\text{K}$

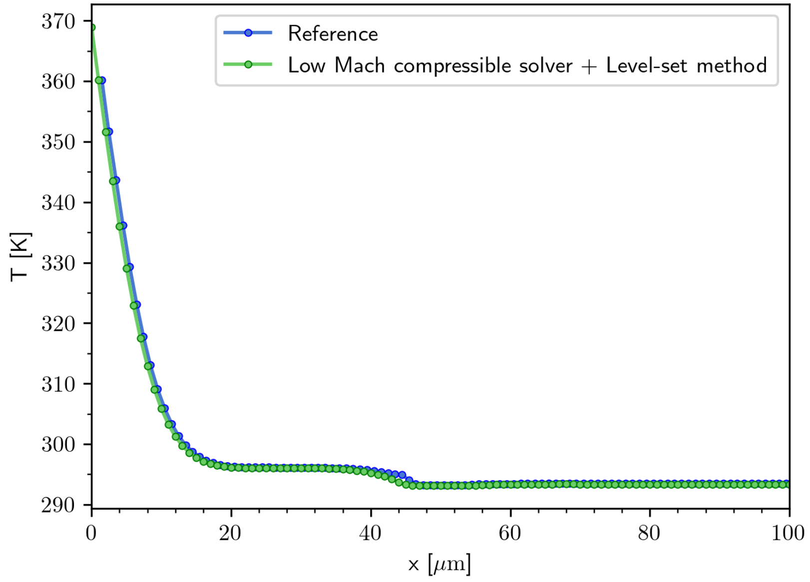

Temperature at $t = 1\mu s$

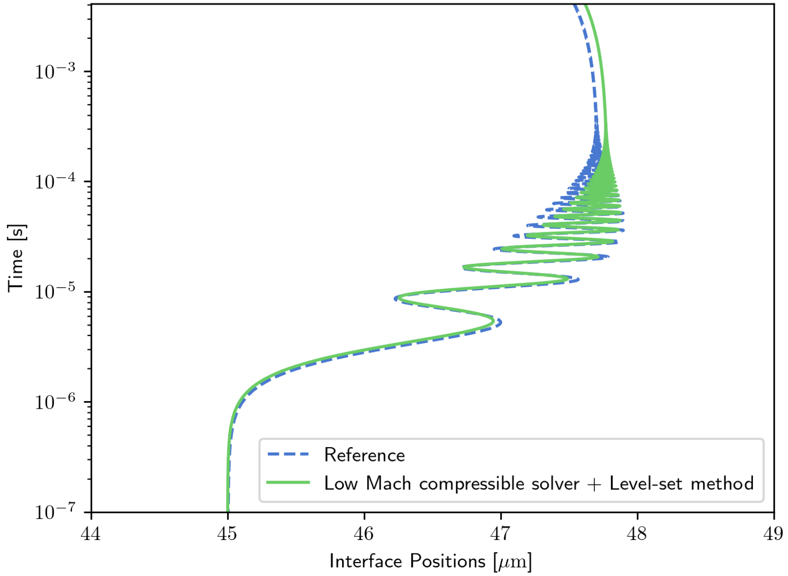

Trajectory of left interface

Reference: ALE, incompressible liquid + compressible gas

Stefan problem $Ja = 2$

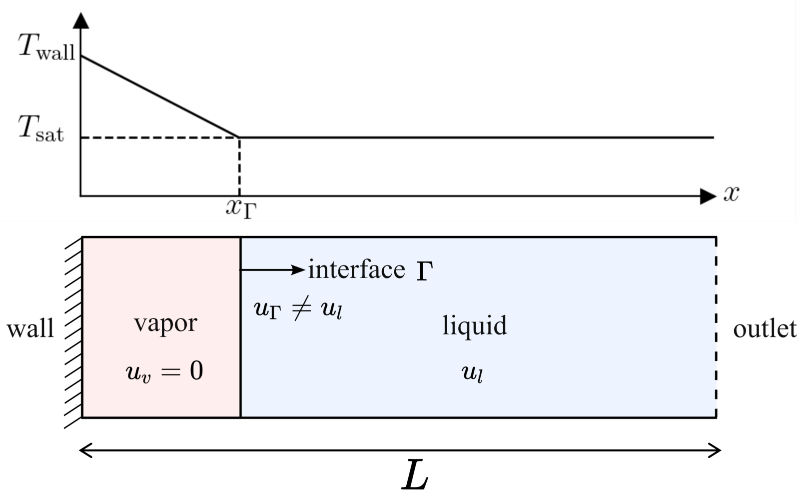

Property	Vapor	Liquid
ρ $(\mathrm{kg \cdot m^{-3}})$	0.25	2.5
μ $(\mathrm{Pa \cdot s})$	0.007	0.098
$\mathcal{K}$ $(\mathrm{W \cdot m^{-1} \cdot K^{-1}})$	0.0035	0.0015
C_p $(\mathrm{J \cdot kg^{-1} \cdot K^{-1}})$	10	10
L_{heat} $(\mathrm{J \cdot kg^{-1}})$	100	
T_{wall} (K)	12	
T_{sat} (K)	10	

$$\rho_{\text{liquid}}/\rho_{\text{vapor}} = 10$$

$$Ja = \frac{\rho_l C_{p,l}(T_{\max} - T_{\text{sat}})}{\rho_v L_{\text{heat}}}$$

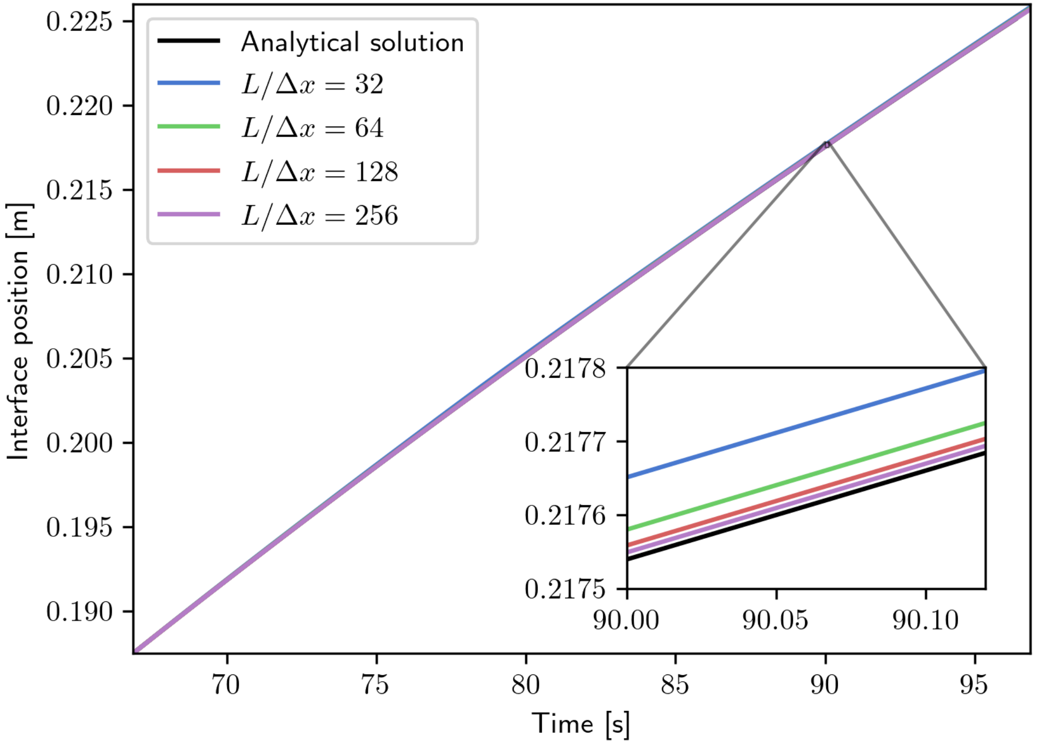

Temporal evolution of interface position x_Γ

Stefan problem $Ja = 30$

Property	Vapor	Liquid
ρ $(\mathrm{kg \cdot m^{-3}})$	0.597	958.4
μ $(\mathrm{Pa \cdot s})$	1.26×10^{-5}	2.80×10^{-4}
$\mathcal{K}$ $(\mathrm{W \cdot m^{-1} \cdot K^{-1}})$	0.025	0.679
C_p $(\mathrm{J \cdot kg^{-1} \cdot K^{-1}})$	2030	4216
L_{heat} $(\mathrm{J \cdot kg^{-1}})$	2.26×10^6	
T_{wall} (K)	383.15	
T_{sat} (K)	373.15	

$\rho_{\mathrm{liquid}}/\rho_{\mathrm{vapor}} = 1600$

$L/\Delta x = 65$

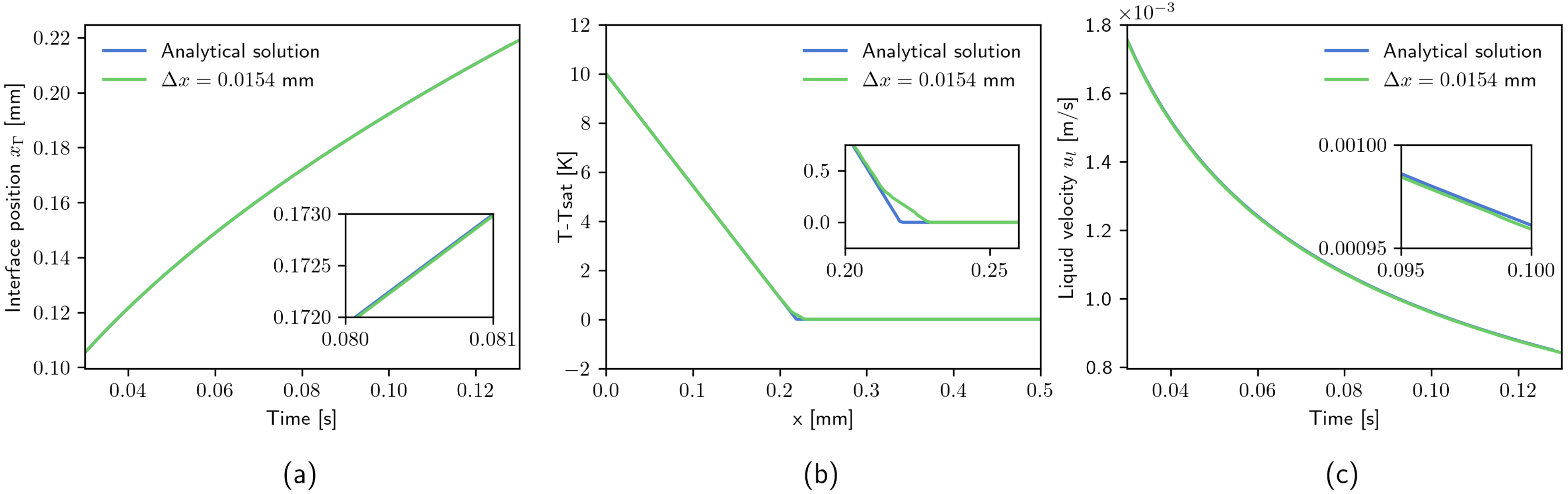

(a)Temporal evolution of the interface position. (b) Temperature profile at t = 0.13 s. (c) Temporal evolution of the liquid velocity.

Mesh refinement strategy

Aim: improve computational efficiency and flexibility

Adaptive Mesh Refinement (AMR)

Based on empirical, a posteriori criteria (gradient, local residuals……)

Multi-Resolution Analysis (MRA)

Based on a rigorous mathematical analysis of wavelet theory.

Use a local wavelet basis whose coefficients provide an accurate measure of the local regularity. Adapt the mesh according to its local regularity.

Implementation

SAMURAI

Structured Adaptive mesh and MUlti-Resolution based on Algebra of Intervals

https://github.com/hpc-maths/samurai

- ✓ C++
- ✓ Able to handle both AMR and MRA
- ✓ @CMAP, École Polytechnique

Multi-resolution example: discretization by point values

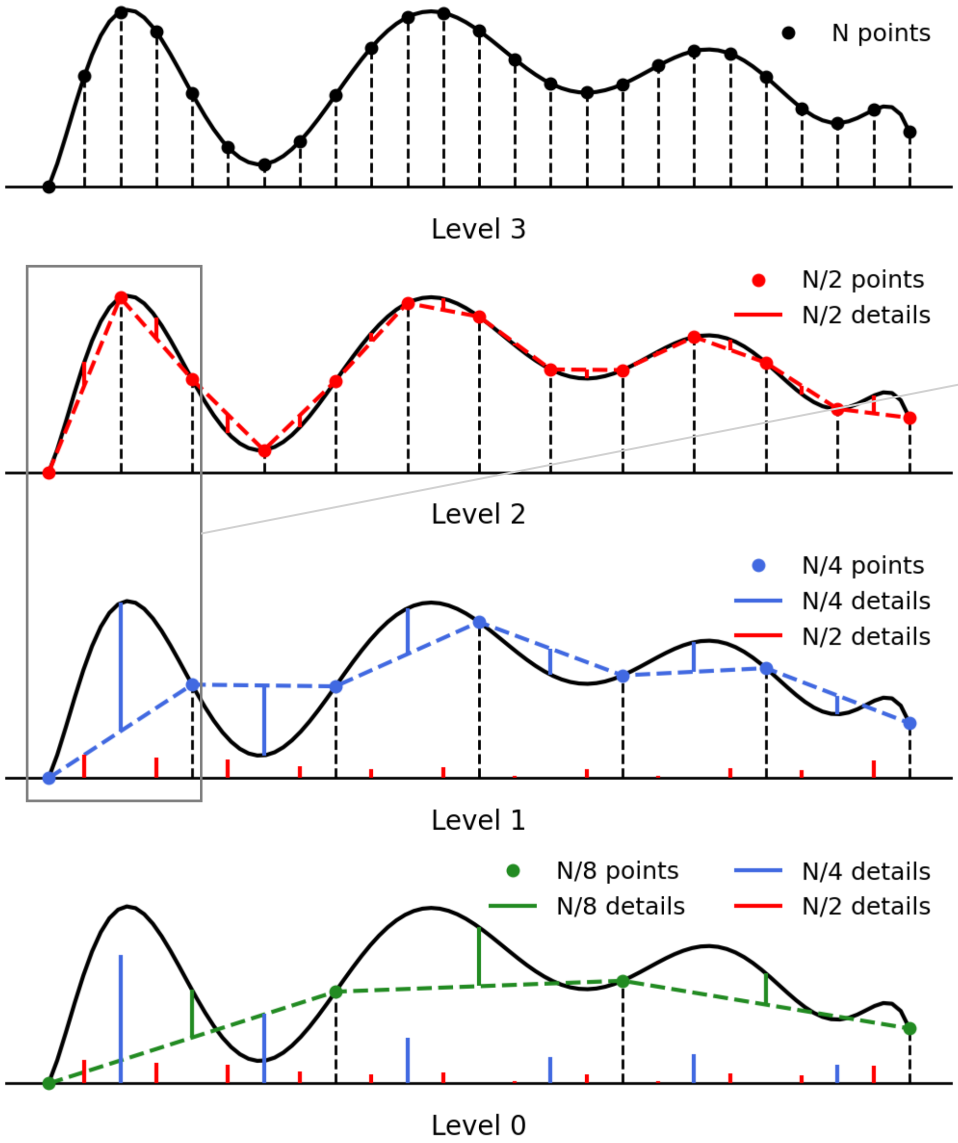

A hierarchy of structured nested grids [M. Postel, 2001]
point-based MR

Aim: approximate solution $\mathbf{v}$ by a piecewise linear function $\hat{\mathbf{v}}$ on a set of intervals

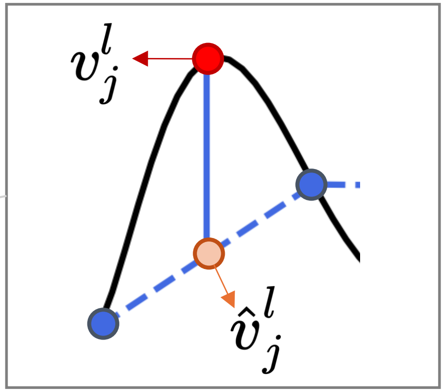

Details

$$d_j^l = v_j^l - \hat{v}_j^l$$

Multiresolution transform

$$\mathbf{v}^L \underset{\mathcal{M}^{-1}}{\overset{\mathcal{M}}{\rightleftharpoons}} (\mathbf{v}^0, \underbrace{\mathbf{D}^1, \ldots, \mathbf{D}^L}_{\text{all vectors of details}})$$

solution on the finest level

solution on the root level

all vectors of details

Refinement criterion

detail > ε threshold parameter at a grid level

Multi-resolution example: 1D function

$$f(x) = 0.5 - |x|$$

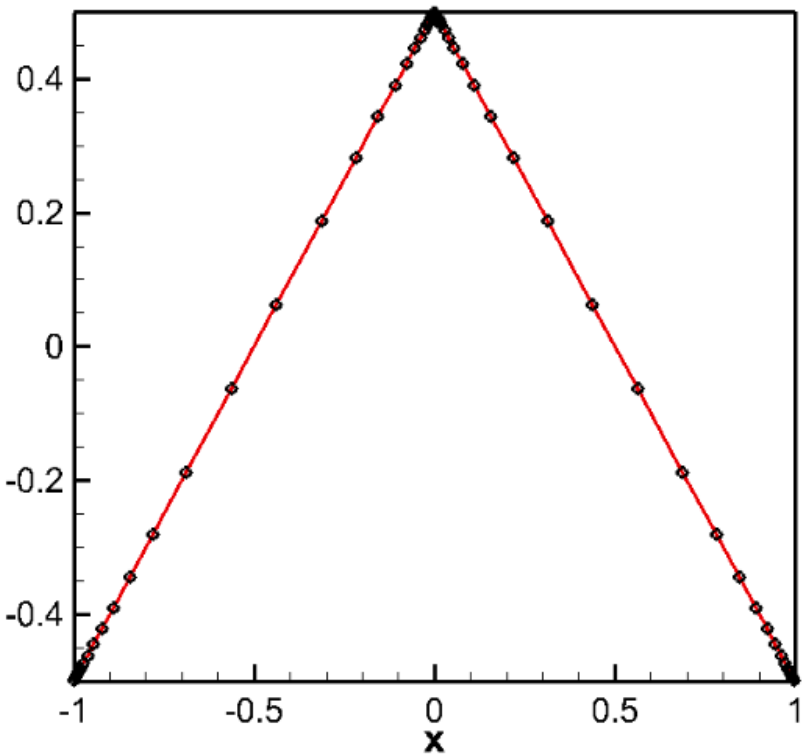

grid level

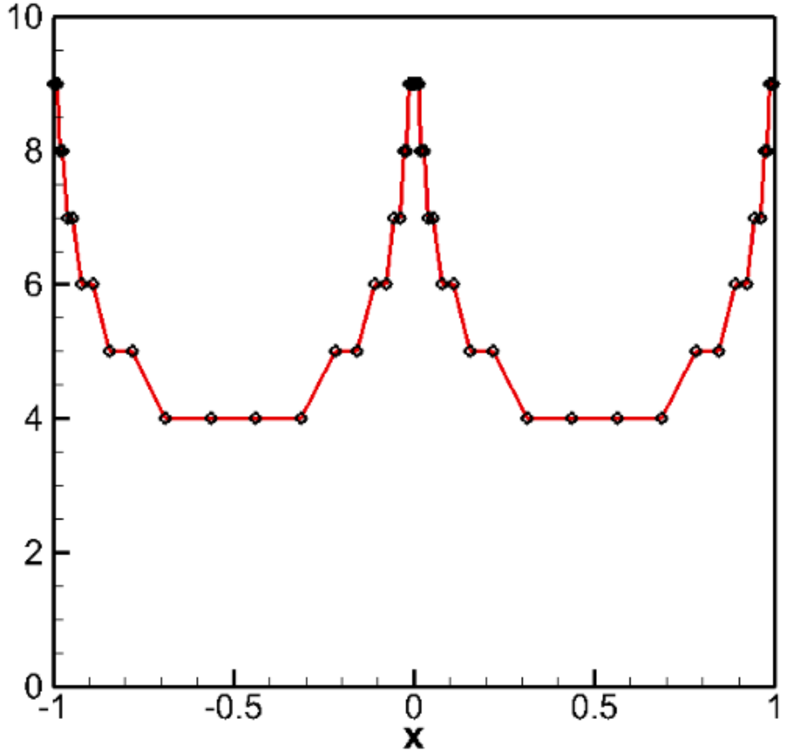

Multiresolution on 1D function [C. Tenaud et al., 2011]

Stefan problem + MR

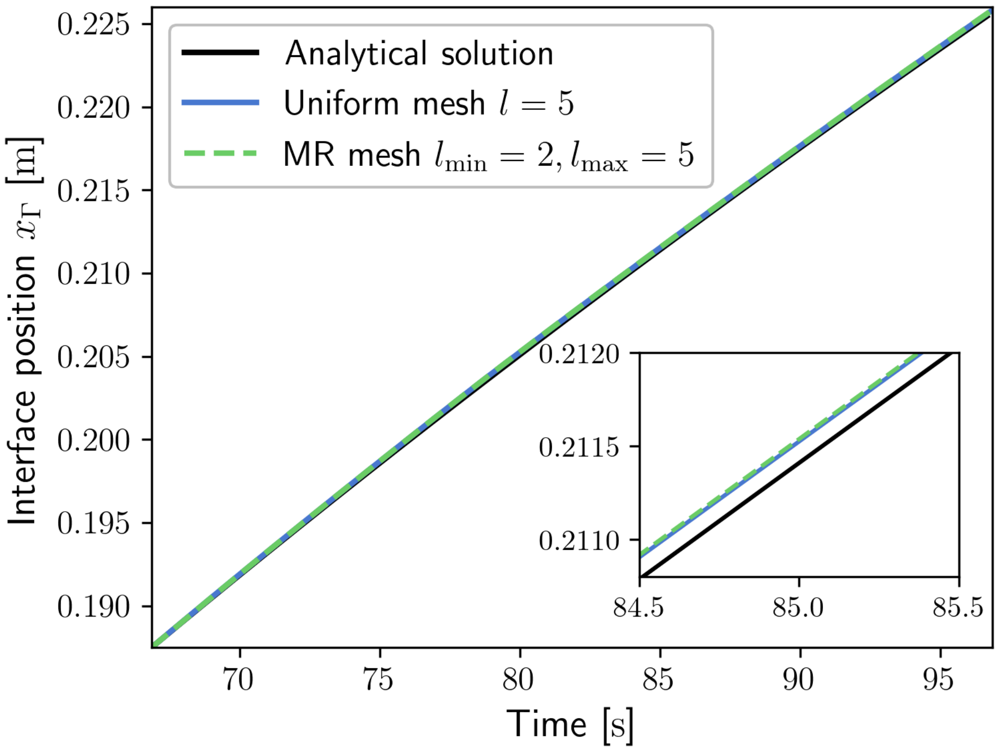

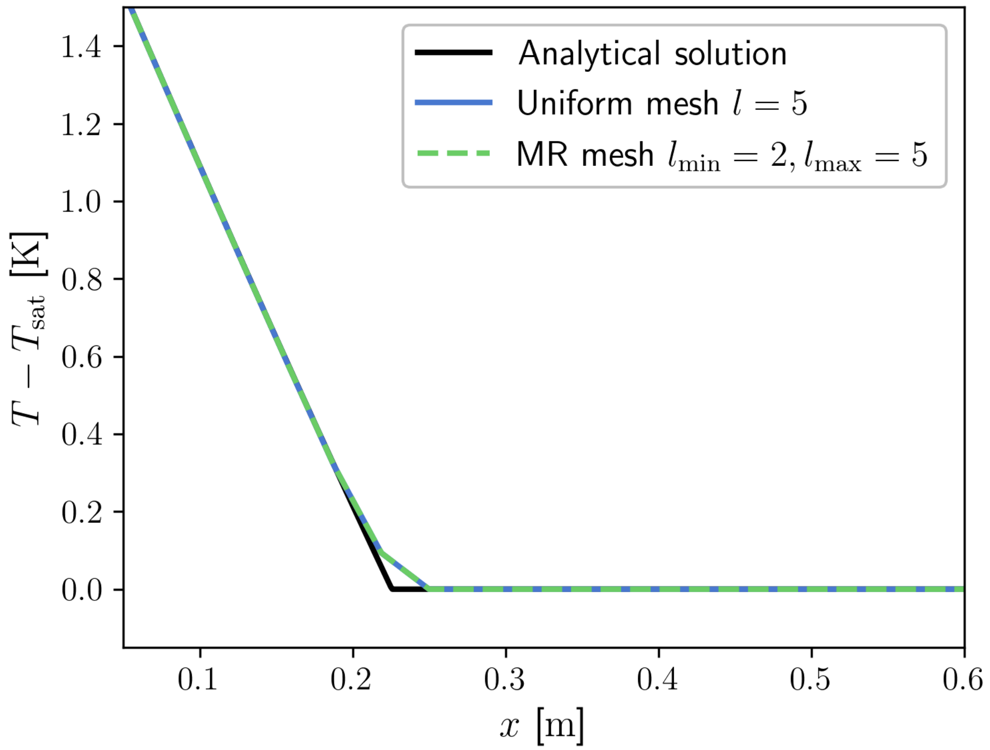

Uniform mesh (grid level 5, 32 grid points) and **MR mesh** (four grid levels [2, 5])

MR mesh for Stefan problem

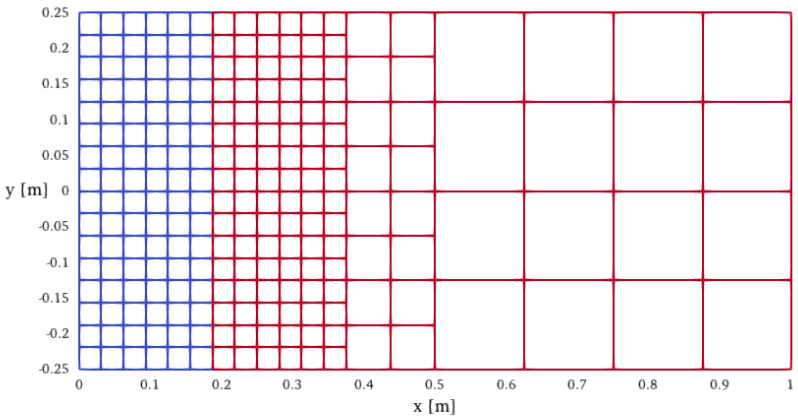

MR mesh [2, 5]

mesh compression rate = 56.3%

$$CR = 1 - \frac{\#\text{cells}_{\text{MR}}}{\#\text{cells}_{l_{\text{max}}}}$$

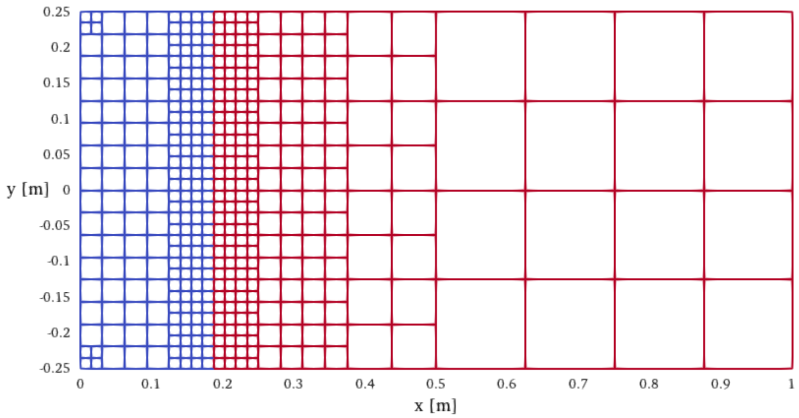

MR mesh [3, 6]

mesh compression rate = 79.4%

$\varepsilon = 0.01, r = 2$

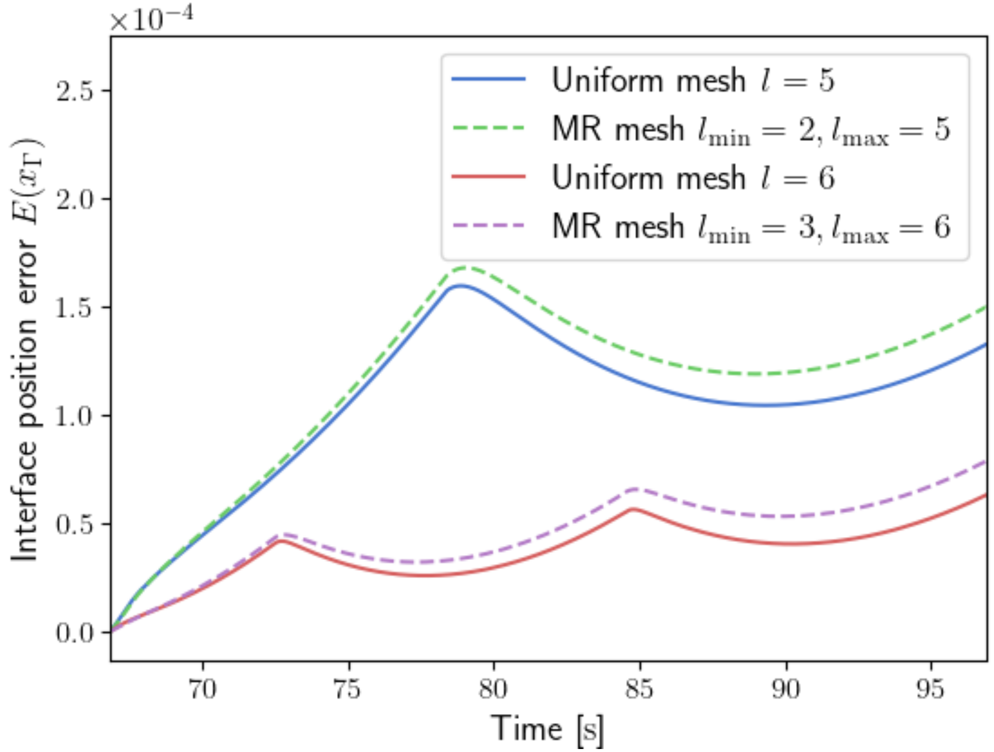

$$E(x_\Gamma) = \frac{|x_{\Gamma,\text{num}} - x_{\Gamma,\text{ana}}|}{L}$$

Local grid refinement

threshold parameter on each grid level l:

$$\varepsilon_l = 2^{N_{\text{dim}} \cdot (l-L)} \varepsilon$$

N_{dim}	dimension
L	the finest grid level
ε	tolerance specified by user

scaled by global maximum :

$$\frac{\left|d_j^l\right|}{\max_j \left|d_j^l\right|} > \varepsilon_l$$

→ Refine the mesh; otherwise, coarsen the mesh

Remark:

- value of $\varepsilon, 0 < \varepsilon \ll 1$ has a leading role in the accuracy and efficiency
- *details* decay with the grid level for smooth solutions, and recover large values in discontinuous regions

[C. Tenaud et al., 2015]

Rayleigh-Taylor instabilities + MR

In practice:

- calculate details based on $[\rho, \rho u, \rho v, \rho E]$
- use tolerance suggested by [B. Bihari and A. Harten, 1997]

$$\varepsilon_l = 2^{(N_{\text{dim}}+r)\cdot(l-L)}\varepsilon \longleftarrow \varepsilon, r$$

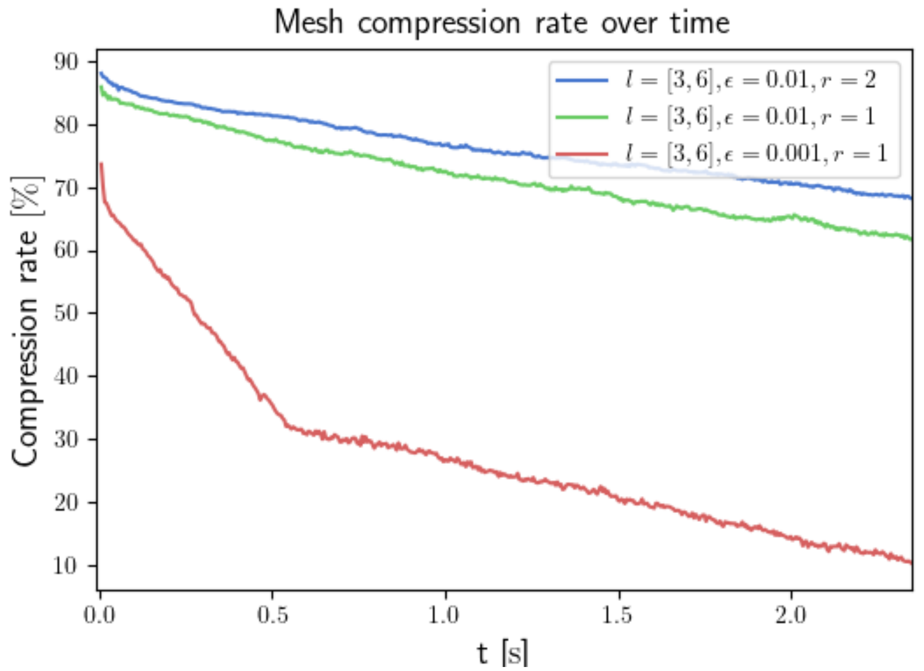

Compromise between accuracy and compression rate

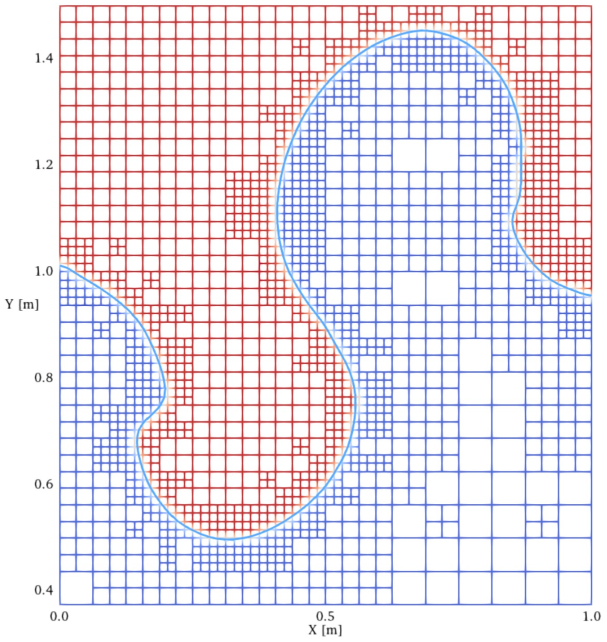

MR mesh $\varepsilon = 0.01, r = 2$

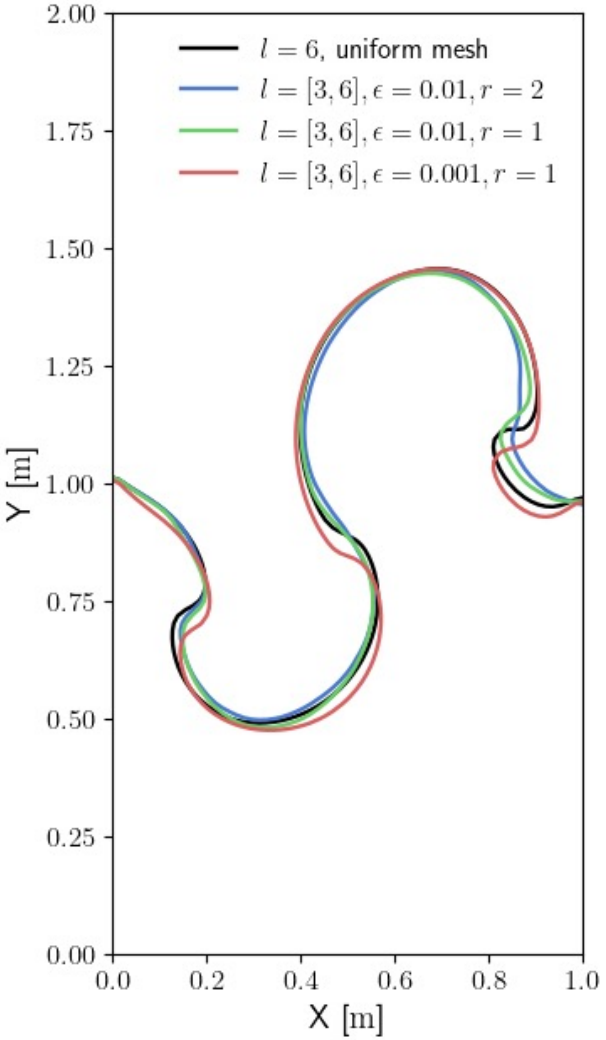

$t^* = 2.35$

Summary and Outlook

Objective:

- ✓ Accurate in interface capturing
- ✓ Accurate in the low Mach regime
- ✓ Capable of handling heat transfer and phase change
- ✓ Integrated with the adaptive mesh refinement technique

A two-fluid compressible solver

- interface is captured by level set method
- with low Mach correction
- with sharp-interface phase change model
- with multiresolution adaptive mesh refinement

Work in progress

- Evaluate the performance of multiresolution (error analysis, computational time, mesh compression)
- Extend to 2D bubble boiling case

Thank you for your attention!
Questions?

gen.wu@upsaclay.fr

Rayleigh-Taylor instabilities + MR

uniform mesh

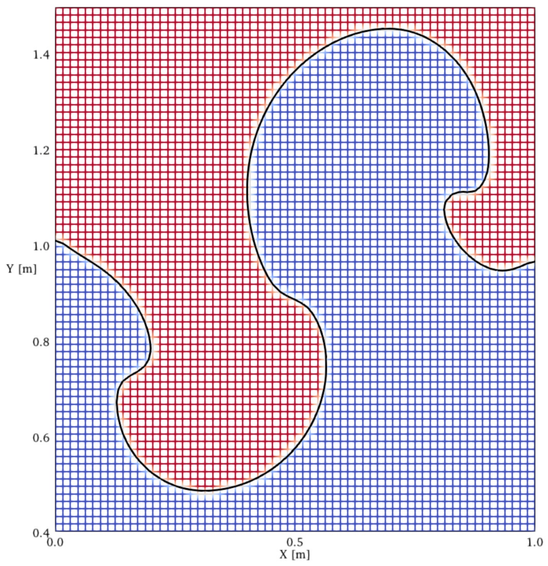

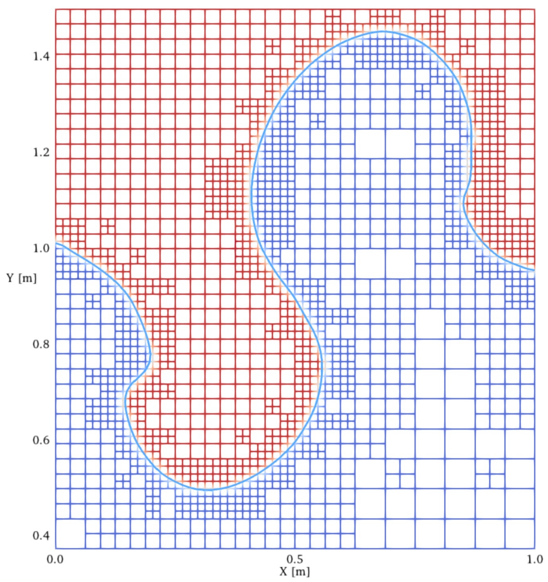

$\varepsilon = 0.01, r = 2$

$\varepsilon = 0.01, r = 1$

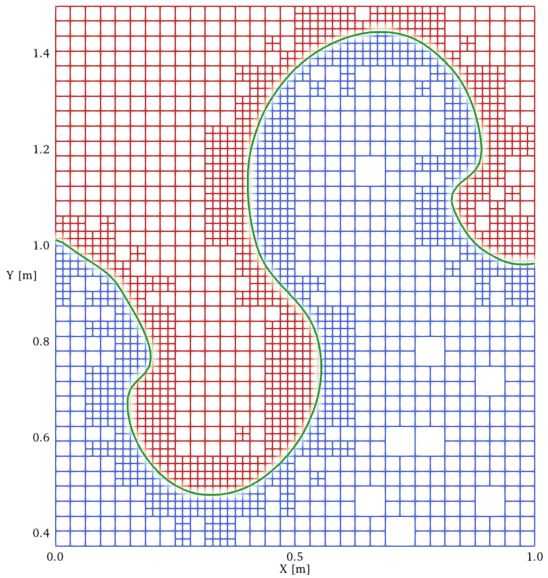

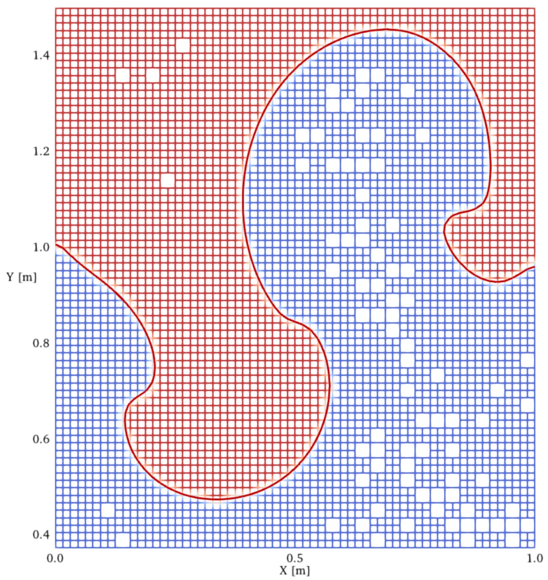

$\varepsilon = 0.001, r = 1$